

Designing and Modeling of Efficient Resonant Photo Acoustic Sensors for Spectroscopic Applications

Fahem Yehya, Anil K. Chaudhary

Advanced Centre of Research in High Energy Materials,

University of Hyderabad, India

E-mail: anilphys@yahoo.com

Received October 2, 2010; revised November 22, 2010; accepted November 25, 2010

Abstract

We report the modeling and designing aspects of different types of photo-acoustic (PA) cell based on the excitation of longitudinal, radial and azimuthal mode using CW and pulse lasers. The results are obtained by employing fluid dynamics equations along with Bessel's function. The obtained results based on stimulation of longitudinal, radial and azimuthally resonance modes of the Photo acoustic signals in the suitable cavity. This is utilized to design highly efficient low volume PA detector for the spectroscopic studies of different types of atmospheric pollutants. We have also studied the dependence of the excited photo acoustic signals on various parameters such as cell radius, laser power, absorption coefficient, quality factor 'Q' along with the first longitudinal, radial, azimuthal mode and the pressure. The simulated results show the linearity of the PA signal with different concentration of the gas sample.

Keywords: Photo Acoustic, Resonance, Cavity, Spectroscopy, Modes

1. Introduction

The photo acoustic effect was first reported by A. Bell (1880), he found that thin disc emit sound when exposed to a rapidly interrupted beam of sunlight [1], in the following years several renowned scientists studied this new phenomena in detail Tyndall [2], Rontgen [3].

But the first application of the effect of trace gas monitoring were reported in the late 1960s because of the two important steps leading to this technique were the invention of the laser as an intense light source and the development of the highly sensitive sound detector such as microphone and lock-in-amplifier for amplification. Kerr and Atwood were the first to apply the laser in photo acoustic signal (PAS) where they used CW (CO₂) laser and they achieved the minimum detectable absorption coefficient α_{\min} the order of 10^{-7}cm^{-1} for CO₂ buffered in N₂, Kreuzer (1971) who reported on the sensitive detection of (CH₄) in N₂ with lowest detection order of 10^{-8} (ppb) using He Ne laser operating at 3.39 nm [4].

Typically non resonant photo acoustic cell of cylindrical shape has been investigated by Sigrist *et al.* [5]. Resonant cell based on excitation of radial, azimuthal and longitudinal modes by different types of lasers are reported by different groups [6-10]. A special feature of

PAS is the fact that the ultimate detection sensitivity depends on several factors such as the amount of energy stored in the absorption sample in the form of heat, size of absorbing sample, cell constant, input laser power and the sensitivity of the microphone [11].

In the PA effect the molecular absorption of photons result in the excitation of molecular energy level, the excited state can released its energy either by radiative process or by non-radiative process (collisional relaxation). As the radiative lifetime of vibrational level are long compared to the time required for collisional deactivation and the photon energy is too small to induce chemical reaction [6]. Thus, the absorbed energy is completely released as heat in the sample as shown in **Figure 1**. In fact this process is generated by two distinct methods [10].

1.1. Modulated Excitation

In modulated excitation scheme, the intensity of the radiation sources periodically modulated in the form of a square or a sine wave using mechanical chopper. The range of modulation frequencies usually lies between few Hz up to several kHz. The resulted pressure fluctuations generate sound waves in the audible range, which can be

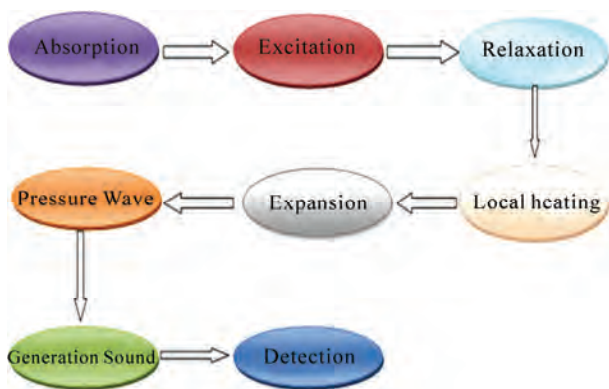


Figure 1. Schematic of generation and detection of photo acoustic signal

detected by microphones. As data analysis is performed in the frequency domain with the help of lock-in amplifiers which enables the simultaneous recording of both amplitude and phase of the sound signal. If the modulated frequency matches with one of the eigen frequency of the cavity, then the cavity cell works as an amplifier.

1.2. Pulse Excitation

However, In case of pulsed PAS, Nano seconds laser pulses are employed to excite the cavity mode. Since the repetition rate is in the range of a few Hz, provides short illumination followed by a longer dark period. Data analysis in this case is performed in the time domain using boxcar average/integrator systems couples with oscilloscope.

Transformation of the signal pulse into the frequency domain generates a wide spectrum range of acoustic frequencies which extended up to the ultrasonic range. Thus, laser beams modulated in the form of a sine wave excite only single acoustic frequency, whereas short laser pulses generate broadband of acoustic signals.

In this work, we have thoroughly studied three different sized cavities and simulated the dependence of photo acoustic signal on several factors such Q-factor, cavity radius, pressure, absorption coefficients, pulse duration of laser along with modulation frequency. The work is divided into three main sections. The first section describes the typical experimental set up for photo acoustic measurement along with calculation details of first four values of resonance frequency of all modes for the three types of cavities.

The second section deals with the estimation of Q-factor of all acoustic cavities correspond to first resonance mode. This help to understand the dependence of photo acoustic signal on Q-factor .In addition, dependence of photo acoustic signal on the cavity radius, laser power and gas concentration are also being studied.

In the last section, we have studied the dependence of photo acoustic signal on pressure and the absorption coefficient along with the first three longitudinal and radial modes of three acoustic cavities.

2. Theory

The inhomogeneous wave equation of the sound pressure in the lossless cylindrical resonator is well explained by different groups [4,12-14].

$$\frac{d^2 P(r,t)}{dt^2} - c^2 \nabla^2 P(r,t) = (\gamma - 1) \frac{dH(r,t)}{dt} \quad (1)$$

where c , γ and H are the sound velocity, the adiabatic coefficient of the gas and the heat density deposited in the gas by light absorption, respectively.

Because the sound velocity which is proportional to the gradient of $P(r)$ vanishes at the cell wall, the $P(r)$ must satisfy the boundary conditions of the vanishing gradient of $p(r)$ normal to the wall [11].

The solution of Equation (1) is given by:

$$P(r,t) = C_0(t) + \sum_{n=0}^{\infty} C_n(t) P_n(r) \quad (2)$$

where $C_0(t)$, $C_n(i)$ are the eigen mode amplitude of corresponding sound wave, $C_n(t)$ is given by the Fourier series as :

$$C_n(t) = \sum_{n,m} A_{n,m} e^{imw_0 t} \quad (3)$$

The dimensionless eigen modes distribution of cylindrical resonator is the solution of the homogeneous wave equation and we can be expressed as:

$$P_n(r,t) = P_n(r) e^{imw_0 t} \quad (4)$$

where W_n is the resonance frequency of the cavity resonator, $P_n(r)$ is:

$$P_n(r) = P_{mq}(r, \varnothing, z) - J_m(K, r) \cos(K_z z) \begin{cases} \cos(m\varnothing) \\ \sin(m\varnothing) \end{cases} \quad (5)$$

And amplitude as:

$$A_n = \frac{iw_0(\gamma - 1)fn}{w_n^2 - w_0^2 + \left(iw_0 \frac{w_n}{Q} \right)} \quad (6)$$

where f_n is the overlap integral which describes the effect of overlapping between the pressure distribution of the nth acoustic resonance frequency and the propagating laser beam divided by the normalized value of the nth eigen mode as:

$$f_n = \frac{\int H(r)P_n(r)dv}{\int Pn^2(r)dv} \tag{7}$$

2.1. The Photo Acoustic Signal (PAS)

The photo acoustic signal (*s*) is given by:

$$S = CP \propto \tag{8}$$

where *C* is the cell constant which can expressed as:

$$C = \frac{(\gamma - 1)f_nIQ}{wV} R_{mic} P_n(r) \tag{9}$$

where *R_{mic}* is the microphone sensitivity (mv/pa), *Q* is the quality factor which physically means the accumulated energy in one period divided by the energy lost over one period, the quality factor can be defined as:

$$Q = \frac{w_0}{\Delta w} \tag{10}$$

w₀ and Δw are the resonance frequency and the half width of the resonance profile (FWHM).

Therefore the minimum detectable absorption coefficient α_{min} is given by:

$$\alpha_{min} = \frac{S_{min}}{CP} \tag{11}$$

where *S_{min}* is the minimum detectable signal:

$$S_{min} = \frac{S_{det}}{S_{mic}} \tag{12}$$

where *S_{det}* is the minimum detectable microphone signal and *S_{mic}* is the microphone responsivity.

The contribution of noise comes from the microphone, background noise, preamplifier, gas flow, and environment ...etc. effect on the value of *S_{min}*, [17] cell constant (*c*) = 175 pa-cm/w, the beam laser power *p* = 10 mw, microphone responsivity *S_{mic}* = 100 mv/pa and the level of the PA detector *S_{det}* = 100 nv - 1 μv, so from (12) the minimum absorption be in the range (5 × 10⁻⁷ - 5 × 10⁻⁹) cm⁻¹. We can also estimate the minimum detectable concentration of the sample by using this expression [4]:

$$C_{min} = \frac{\alpha_{min}}{N_{tot}\sigma} \tag{13}$$

For, $\alpha_{min} = 10^{-8} \text{ cm}^{-1}$, $N_{tot} = 10^{19} \text{ cm}^{-3}$, $\sigma = 10^{-8} \text{ cm}^{-1}$ the minimum detectable concentration is $C_{min} = 10^{-9}$ this means in the ppb range.

The PAS for longitudinal and radial for different value of *n* and α can be written as [16,17]:

$$PAS_j(r_M, v_j) = [(\gamma - 1)/2\pi v_j] f_n(v_j) \left[\frac{P}{V} \right] \begin{cases} 2(-1)^{\frac{n_x}{2}} \frac{(1 - e^{-\alpha l})}{1 + \left(\frac{n_x \pi}{\alpha L}\right)} & \text{longitudnal mode(14) - A} \\ \left(\frac{1}{J_0(x_{0n})}\right) (1 - e^{-\alpha l}) & \text{radial mode(14) - B} \end{cases}$$

3. Results and Discussion

It is divided into three parts, the first part deals with the experimental layout whereas second part deals with effect of quality factor on PAS and third parts comprises the effect of pressure on PAS.

3.1. Typical Photo Acoustic Set Up for PA Measurement

Figure 2 shows the typical experiment set up for recording the PAS exited by lasers. Where we are using a chopper for modulating the incident laser beam if CW laser is employed in place of pulsed laser, the different types of acoustic filter which can used to reduce the external noise, the resonance cavity which is made of stainless steel and its first resonance frequencies in the range of the chopper values, a microphone coupled with lock-in-amplifier for CW laser or with boxcar average

and oscilloscope in the case of pulsed laser.

3.2. Resonance Frequencies

When the laser beam directed along the lossless cylindrical resonator axis, the eigen frequencies *f_{mnq}* of the

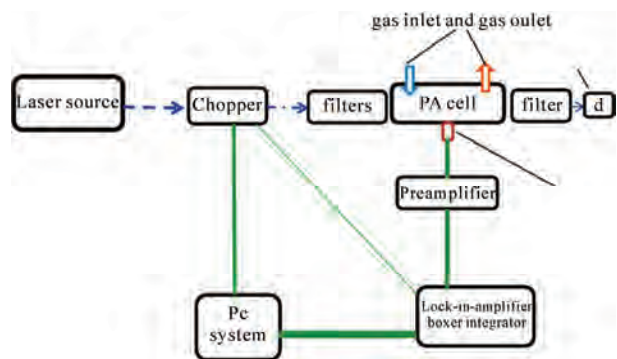


Figure 2. The typical set up for PA measurement.

acoustic normal modes is given by:

$$F_{mq} = c/2 \left(\left(\frac{\alpha_{\min}}{R} \right)^2 + \left(\frac{q}{l} \right)^2 \right)^{\frac{1}{2}} \quad (15)$$

α_{\min} is the n th root of the $dJ_m/dr = 0$ at $r = R_0$ divided by π . R, L are the radius and length of the cavity resonator and C is the sound velocity.

The indices $n = 0, 1, 2, \dots, m = 0, 1, 2, \dots, q = 0, 1, 2, \dots$ refer to the eigen values of the radial, azimuthal and longitudinal modes.

3.2.1. Frequencies Resonators for Longitudinal Modes

We calculated the first resonance frequency of all modes (*i.e.* longitudinal, radial, azimuthally) for three different size cavities.

In the longitudinal mode the indices $n = m = 0$ and the resonance frequencies can be calculated from this equation

$$f_{00q} = qc/2l \quad (16)$$

The values of the longitudinal frequencies are shown in the **Table 1**, and from Equation (5) the eigen mode function will be as:

$$P_n(r) = P_{00q}(z) = \cos(K_z z) \quad (17)$$

The simulation of the first four patterns of frequency modes is shown in **Figure 3**.

3.2.2. Frequency Resonators for Radial Modes

In the radial modes the indices m and $q = 0$ and the resonance frequencies is calculated by using

$$f = c\alpha'(0n)/2\pi r \quad (18)$$

And the Eigen modes distribution will be as:

$$P_n(r) = P_{0n0}(r) = J_m(k_r r) \quad (19)$$

The values of the radial frequencies and their corresponding pattern are shown in the **Table 2** and in **Figure 4**.

3.2.3. Frequency Resonators for Mixture Radial and Azimuthal Modes

In the case of radial and azimuthal modes the indices $q = 0$ and the resonance frequencies are calculated by using:

$$F_{mn0} = c\alpha'(mn)/2\pi r, (n = 1) \quad (20)$$

And the Eigen modes distribution will be as:

$$P_n(r) = P_{mn0}(r, \varnothing) = J_m(K_r r) \begin{Bmatrix} \cos(m\varnothing) \\ \sin(m\varnothing) \end{Bmatrix} \quad (21)$$

The values of the frequencies and their corresponding pattern are shown in the **Table 3** and in **Figure 5**.

Table 1. The longitudinal resonance frequency for three cavities (f_{00q}).

q	The $C_0 = 336$ m/s, $l = 15$ cm, $r = 4.5$ cm	$C_0 = 313$ m/s, $l = 2.9$ cm, $r = 0.3$ cm	$C_0 = 360$ m/s, $l = 10$ cm, $r = 30$ cm
	The frequency (Hz) First cell	frequency (kHz) Second cell	frequency (kHz) Third cell
1	1120	5.397	600
2	2240	10.793	1200
3	3360	16.190	1800
4	4490	21.586	2400

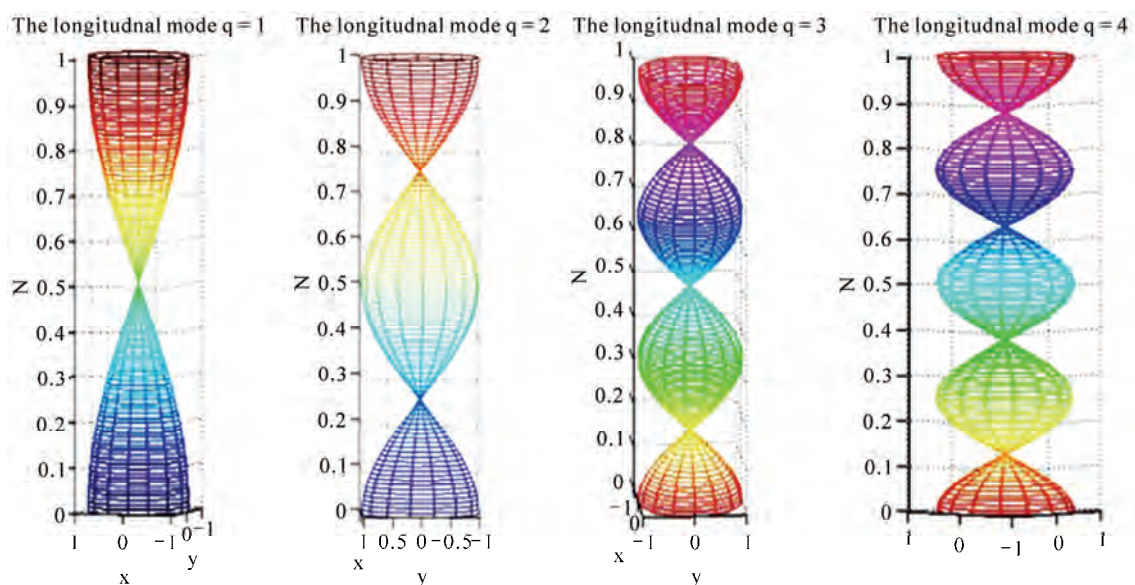


Figure 3. The first four patterns of longitudinal modes.

Table 2. The radial resonance frequencies for three cells.

<i>n</i>	The frequency (Hz) (First cell)	frequency (kHz) (Second cell)	frequency (kHz) (Third cell)
	The $C_0 = 336$ m/s, $l = 15$ cm, $r = 4.5$ cm	$C_0 = 313$ m/s, $l = 2.9$ cm, $r = 0.3$ cm	$C_0 = 360$ m/s, $l = 30$ cm, $r = 10$ cm
1	4553	68.3	2.05
2	8337	125.1	3.75
3	12090	181.3	5.44
4	15833	237.5	7.125

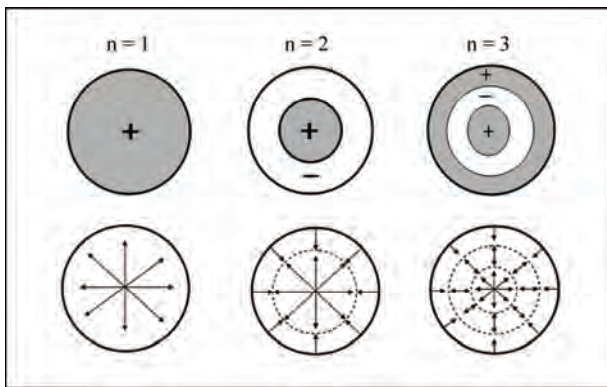


Figure 4. The first three patterns of radial modes.

Table 3. The resonance frequencies of both radial and azimuthal.

<i>m</i>	The frequency (Hz) (First cell)	frequency (kHz) (Second cell)	frequency (kHz) (Third cell)
	The $C_0 = 336$ m/s, $l = 15$ cm, $r = 4.5$ cm	$C_0 = 313$ m/s, $l = 2.9$ cm, $r = 0.3$ cm	$C_0 = 360$ m/s, $l = 30$ cm, $r = 10$ cm
1	6335	95.02	2.850
2	7969	119.5	3.586
3	9525	142.87	4.286

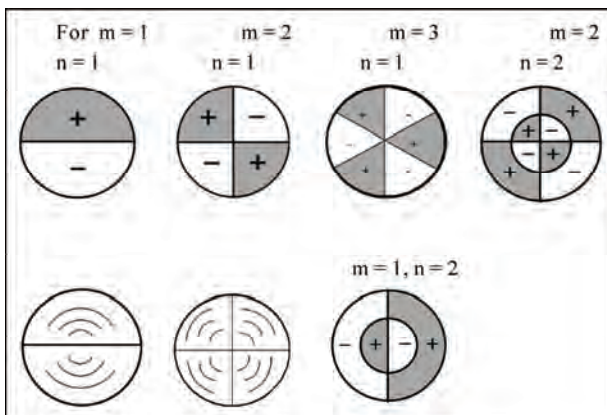


Figure 5. The radial and azimuthally patterns.

In case of radial and azimuthal modes the excited frequency of the smallest cavity resonator are much higher than that for other cavities.

3.3. The Effect of the Quality Factor “Q” on the Profile of Eigen Frequency and PAS

The cavity resonance having cross section in the range of centimeters usually has high-Q for cavity eigen modes [12]. In general, the typical quality factor is determined from the profile of the Eigen mode of the resonance cavity by using Equation (11). But this can also be estimated by considering different type of losses of the cavity [13, 15].

From equation [6], it is very much clear that the amplitude of the resonance frequency can be enhanced by increasing the Q-factor which can only be achieved by decreasing the losses of the cavity. P. Hess *et al.* reported that the smoothness of the internal surface of cavity plays very important role to stabilize the profile of the excited mode along with position of maxima and minima. Therefore, it can easily be achieved by polishing the internal surfaces and attaching acoustic filters as an external buffers at the end of the cavity along with selection of high acoustic impedance microphone.

Figures 6(a), (b) and (c) show the effect of the Q-factor on the photo acoustic signals at first resonance frequency for three different modes *i.e.* longitudinal, azimuthal and radial, respectively for first cell of ($R = 4.5$ cm., $L = 15$ cm.). The corresponding frequency is also mentioned in Table 3 It is very much clear that the longitudinal modes with high Q provides the highest photo acoustic signal.

Figures 7(a), (b) and (c) describe the effect of Q-factor on the photo acoustic signal of the second cell ($R = 3.0$ mm, $L = 2.9$ cm.). It is very much clear that the strength of the PAS related to high Q longitudinal mode shows superiority over the corresponding PAS of radial and azimuthal modes.

For the third cell ($R = 10.0$ cm, $L = 30.0$ cm.), the graphs between Q-factor Vs. PAS are shown in Figures 8(a), (b) and (c) respectively. We find that the strength of photo acoustic signal is much higher than the signal from other two cavities. But it also to be noted that the effect of different types of losses are being neglected (the detailed study is communicated in another paper). These losses are directly proportional to the cavity size. Therefore, large sized cavity will always have more losses than the small sized cavity. In addition, the cell constant inversely proportional to the cavity volume which is described in Figure 10. This shows the superiority of small sized cavity over the large sized cavity.

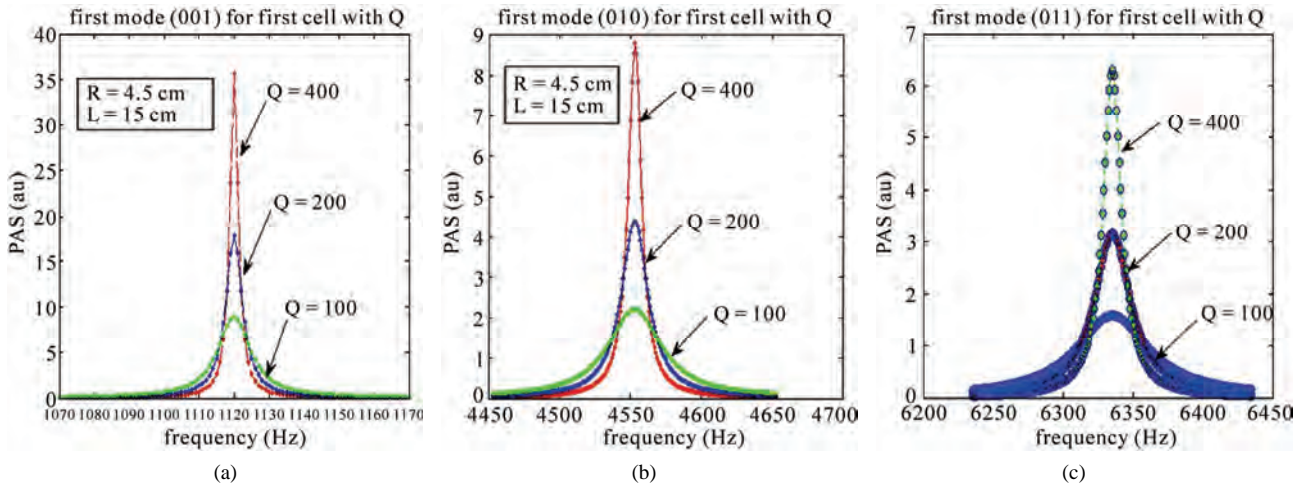


Figure 6. Photo acoustic signal at first resonance frequency for all modes for different Q-factor (a), (b), (c) are the first longitudinal, radial and azimuthal resonance frequency for a first.

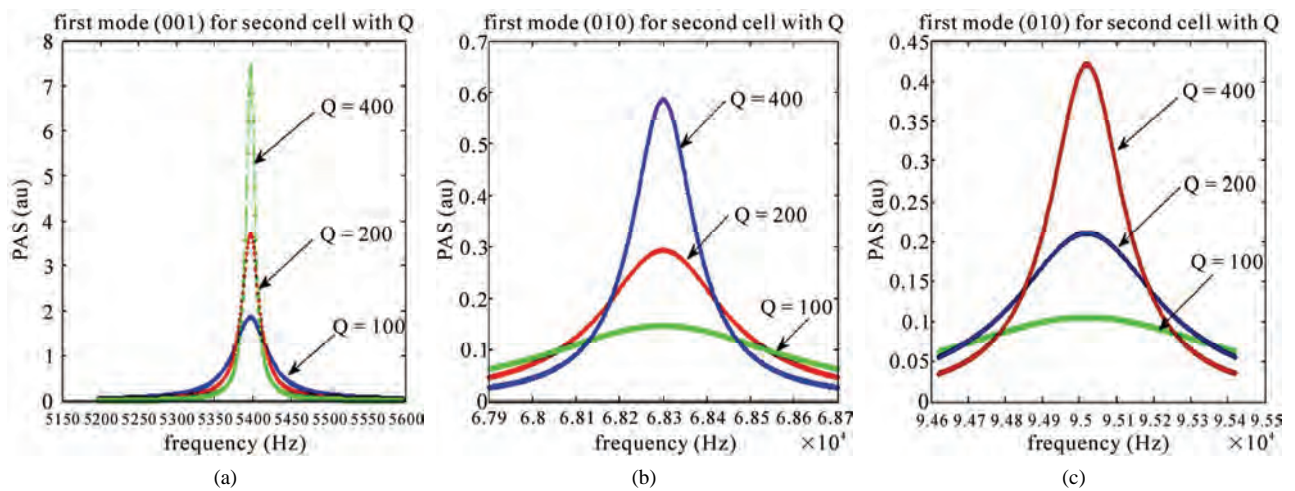


Figure 7. Photo acoustic signal at first resonance frequency for all modes for different Q-factor (a), (b), (c) are the first longitudinal, radial and azimuthal resonance frequency for a second cell.

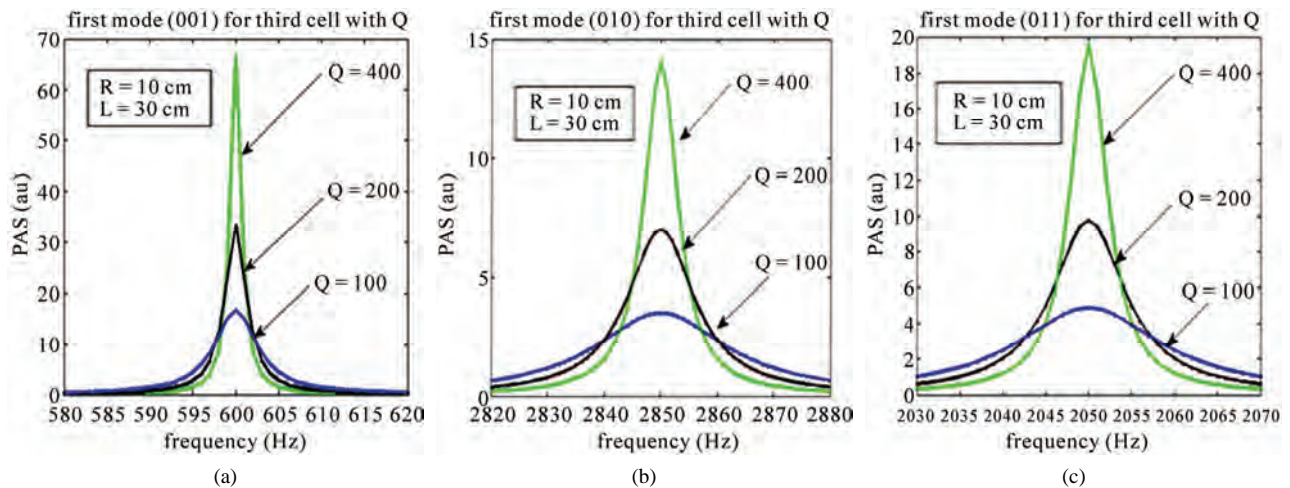


Figure 8. Photo acoustic signal at first resonance frequency for all modes for different Q-factor (a), (b), (c) are the first longitudinal, radial and azimuthal resonance frequency for a third cell.

Figures 9(a), (b) and (c) respectively, show the graph between photo acoustic signals versus Q-factor for the first longitudinal resonance frequency of the three cavities. It show that we can use any of the three cells but with different value of photo acoustic signal, But in case of small sized cell, the azimuthal and radial PAS strength is much more lower than the others two. However, in this case spaital variation along the cavity length is due to excitation of longitudinal modes only. This is popularly known as one-dimensional pipe with low Q-factor.

3.4. The Effect of Laser Parameters and Cavity Dimension on PA Signal

The PAS is inversely proportional to the cavity volume which means that the by decreasing the cavity radius or length one can enhance the photo acoustic signal. We have already elaborated the photo acoustic cell with radius equal to several centimeters along with different

types of modes (*i.e.* longitudinal, radial, azimuthally). In this section we have discussed the solitary case for which cross section dimensions of the cavity is much smaller than the acoustic wavelength which is useful for intra cavity operation.

Figure 11 shows the simulated results of dependence of photo acoustic signal on the radius of three different cells using laser power of the order of 12mW. One can easily see from the graph *i.e.* dash line which represent the smallest cell (one-dimension pipe) is the more efficient than other cells.

Similarly, the dependence of the photo acoustic signal on the laser power has also been simulated and shown in the Figures 11(a) and (b), respectively. The linear nature of the photo acoustic signal with respect to incident laser power clearly indicates that the pulsed resonant PA cell is superior than the CW modulated PA cell. Because, pulsed laser carries high energy resulting very high peak power which also helps to stabilize the frequency with

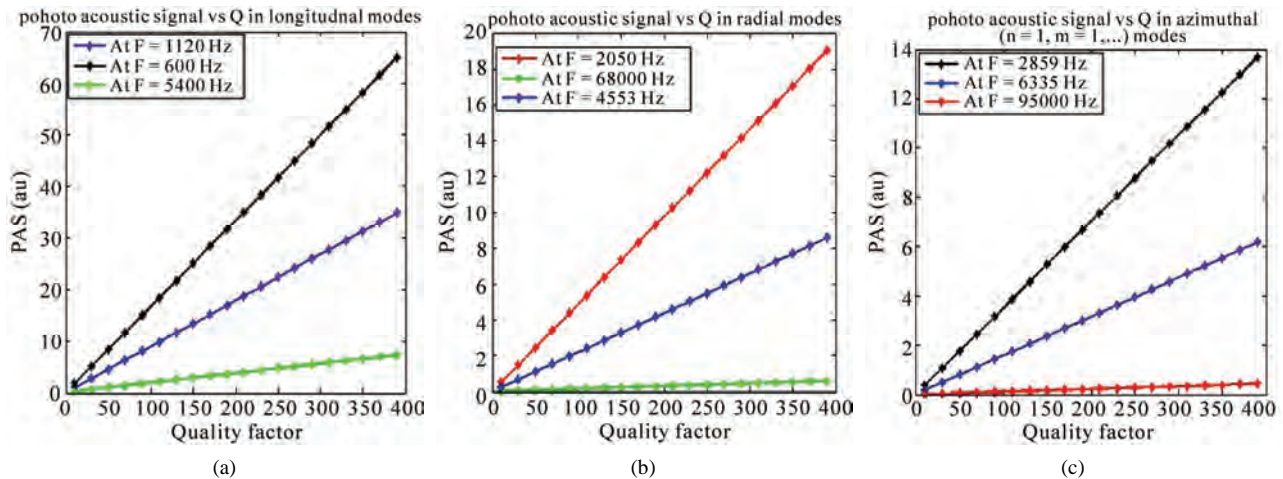
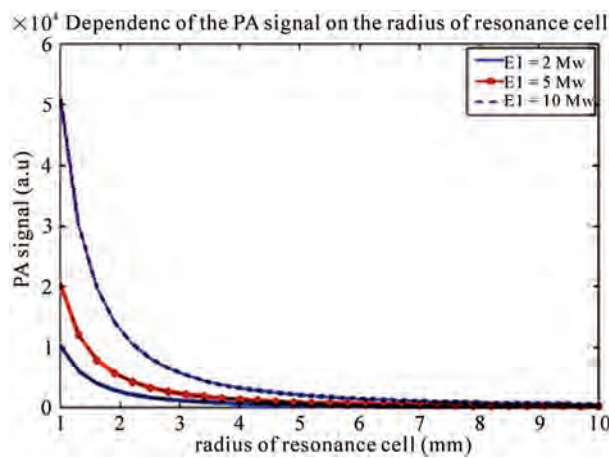


Figure 9. (a), (b) and (c) show the photo acoustic cell vs. Q-factor for longitudinal, radial and azimuthal mode for all cavities.

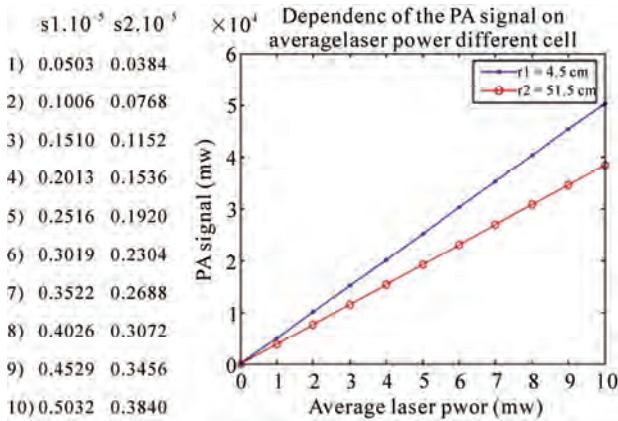
s1	s2	s3
1.0186	2.0372	5.0930
0.4527	0.9054	2.2635
0.2546	0.5093	1.2732
0.1630	0.3259	0.8149
0.1132	0.2264	0.5659
0.0832	0.1663	0.4158
0.0637	0.1273	0.3183
0.0503	0.1006	0.2515
0.0407	0.0815	0.2037
0.0337	0.0673	0.1684
0.0283	0.0566	0.1415
0.0241	0.0482	0.1205
0.0208	0.0416	0.1039
0.0181	0.0362	0.0905
0.0159	0.0318	0.0796
0.0141	0.0282	0.0705
0.0126	0.0252	0.0629
0.0113	0.0226	0.0564
0.0102	0.0204	0.0509

(a)

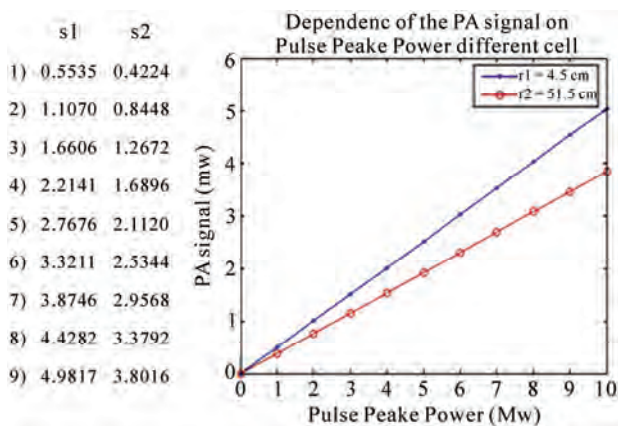


(b)

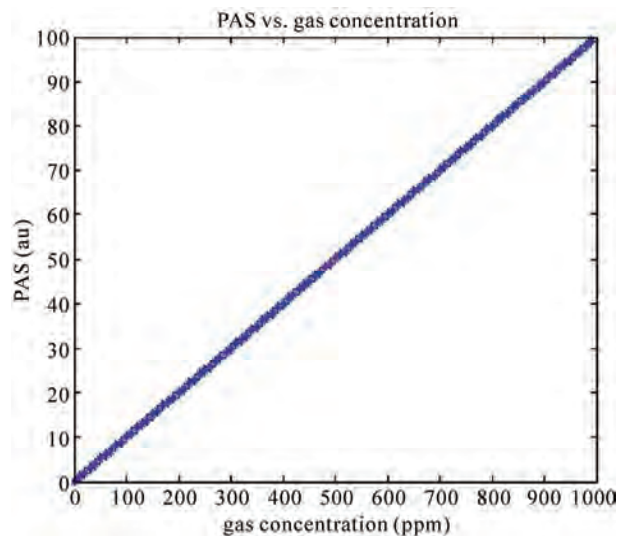
Figure 10. (a) The photo acoustic signal (au) for three cavities; (b) the photo acoustic signal dependence on different radius.



(a)



(b)



(c)

Figure 11. (a) The photo acoustic signal(au)for three cavities and the photo acoustic signal dependence on average laser power; (b) The photo acoustic signal(au) for three cavities and the photo acoustic signal dependence on pulse peak power; (c) The effect of the concentration of gas on the photo acoustic signal.

negligible effect of “Q” value. Pulsed laser also help to excite all the exiting modes at a time.

Figure 11(c) shows the graph between PA signal Vs. Concentration of the gas which is linear in nature and PAS strength increases with the concentration of gas.

3.5. Dependence of the PA Signal on the Average Modulated Laser Power

Equation (8) clearly shows the linear behavior of the PA signal with respect to the incident input laser power which is shown in **Figure 11(a)** for CW laser source.

3.6. Dependence of the PA Signal on Pulsed Peak Power

Figure 11(b) shows the linear behavior of the PA signal with respect to the incident pulse laser E, The strength of the PA signal gets enhanced with enhanced input laser power.

3.7. Dependence of Photo Acoustic Signal on the Concentration of a Sample Gas

Figure 11(c) clearly shows that the signal is increasing linearly with increase of the gas concentration. However, for some gases this linearity can be maintained up to certain limit as a factor of increasing the concentration of the sample gas which ultimately reduces the signal beyond certain concentration due to adsorption of sample gas on the walls of cell.

3.8. Third Part: The First Three Longitudinal Modes vs. Pressure

Figures 12(a), (b) and (c) show the Pressure dependence of the PAS which is plotted after optimizing the overlapped integral factor F_t which also represent the interaction between laser beam and frequency modes .The value of F_t has been optimized to the unity by considering each specific location of eigen modes and suitable laser beam intensity at specific resonance frequency for the given photo acoustic detector. From Equation (15) it is very much clear that photo acoustic signal explicitly depends on the absorption coefficient α which means that the PA signal depends on the amount of optical power absorbed by the gas which is linear in nature with change of pressure of buffer gas. **Figures 12(a), (b) and (c)** show the photo acoustic dependency on the pressure at first three longitudinal modes for three different cavities. There are two distinguish pressure regions, out of which the in the first pressure region PA signal increases drastically with ascending value of pressure which is due to the change

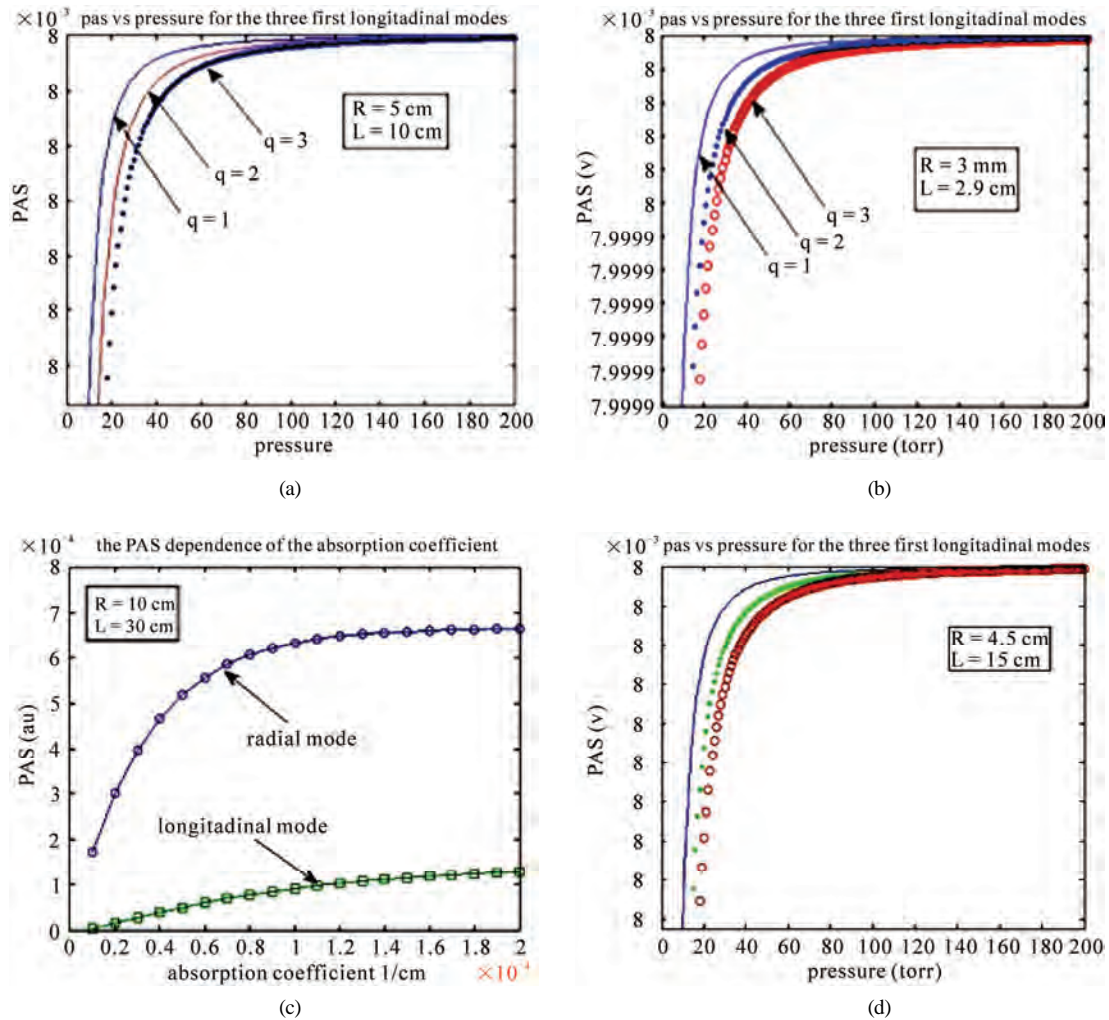


Figure 12. The simulation of photo acoustic signal Vs pressure for the first three longitudinal modes (a) L = 10 cm, R = 5 cm (b) L = 2.9 cm, R = 3 mm (c) L = 15 cm, R = 4.5 cm (d) the dependence of PAS on the absorption coefficient with R = 10 cm, L = 30 cm.

of concentration and fast relaxation from excitation states. While the second pressure region appears just after first region, where photo acoustic signal almost get saturated due to dominating effect of collision broadening.

The dependence of PA signal on varying pressure is not similar for all resonance frequency because each resonance frequency has its own pressure which is responsible for getting saturation point for each one of them independently.

Figure 12(d) shows the dependence of PAS on the absorption coefficient for the first longitudinal and radial modes for the third cell (R = 10.0 cm, L = 30.0 cm).

4. Conclusions

We have successfully simulated the designing aspects of different types of resonant photo acoustic systems/cells for trace gas monitoring. The calculated values of reso-

nance frequencies for longitudinal, radial and azimuthally modes for three different types of cavity resonators show that the reduced volumes of the resonator enhances the efficiency of the sensor. In addition, simulation results also show that at radial and azimuthal modes related to the smallest cavity resonators are much higher than that for other cavities. In present work, we have successfully demonstrated the feasibility aspects based on the dimension of the resonant cavity along with their limitations. For small sized cavity to it is difficult to detect PAS produced by excited radial and azimuthal modes. In addition, the small sized PA cell has the cross section of the cavity resonator smaller than the acoustic wavelength as a result the excited field appears as a spatial variation along the cavity and treated as one dimensional pipe. Also the variation of pressure a, cavity radius, laser power and absorption coefficients along with the detection concentration have been studied.

5. Acknowledgements

Authors gratefully acknowledge the DST, SERC Project LOP-13 Govt, of India and DRDO, Ministry of Defense Govt, of India for financial support. We also acknowledge the fruitful advice from Prof. S. P. Tewari, ACRHEM, University of Hyderabad, Hyderabad (A.P.), India.

6. References

- [1] A. G. Bell, "On the Production and Reproduction of Sound by Light," *American Journal of Science*, Vol. 5, No. 118, 1880, pp. 305-324.
- [2] J. Tyndall, "Action of an Intermittent Beam of Radiant Heat upon Gaseous Matter," *Proceedings of the Royal Society*, Vol. 31, No. 307, 1881. pp. 307-317.
- [3] W. C. Rontgen, "U'berTo'ne, Welchedurchintermittierende Bestrahlungeines Gases Entstehen," *Annual Review of Physical Chemistry*, Vol. 1, No. 155, 1881.
- [4] W. M. Sigrist, "In Air Monitoring by Spectroscopic Techniques," John Wiley and Sons, New York, 1994.
- [5] I. G. Calasso, V. Funtov and M. W. Sigrist, "Analysis of Isotopic CO₂ Mixtures by Laser Photo Acoustic Spectroscopy," *Applied Optics*, Vol. 36, 1997, pp. 3212-3216. [doi:10.1364/AO.36.003212](https://doi.org/10.1364/AO.36.003212)
- [6] A. Thöny and M. W. Sigrist, "New Developments in CO₂-Laser Photo acoustic Monitoring of Trace Gases," *Infrared Physics & Technology*, Vol. 36, No. 2, 1995, pp. 585-615.
- [7] A. Petzold and R. Niessner, "Photo Acoustic Sensor for Carbon Aerosols," *Applied Physics Letters*, Vol. 66, No. 10, 1995, pp. 1285-1297. [doi:10.1063/1.113271](https://doi.org/10.1063/1.113271)
- [8] Z. Bozóki, A. Mohácsi, V. Szabó, Z. Bor, M. Erdélyi, W. Chen and F. K. Tittel, "Near-Infrared Diode Laser Based Spectroscopic Detection of Ammonia: A Comparative Study of Photo acoustic and Direct Optical Absorption Methods," *Application Spectrosc*, Vol. 56, No. 6, 2002, pp. 715-719.
- [9] A. Boschetti, D. Bassi, E. Iacob, S. Ionnatta, L. Ricci and M. Scotoni, "Resonant Photo Acoustic Simultaneous Detection of Methane and Ethylene by Means of a 1.63- μ m Diode Laser," *Applied Physics B*, Vol. 74, No. 3, 2002, pp. 273-278. [doi:10.1007/s003400200790](https://doi.org/10.1007/s003400200790)
- [10] S. Thomas, "Photo Acoustic Spectroscopy for Process Analysis" *Analytical and Bioanalytical Chemistry*, Vol. 384, No. 5, 2006, pp. 1071-1086.
- [11] S. Tapio, M. Albert, T. Juha, S. Jaakko and H. Rolf, "Resonant Photo Acoustic Cell for Pulsed Laser Analysis of Gases at High Temperature" *Review scientific Instruments*, Vol. 80, No. 12, 2009, p. 123103.
- [12] A. Miklos, P. Hess, "Application of Acoustic Resonators in Photo Acoustic Trace Gas Analysis and Metrology" *Review scientific Instruments*, Vol. 72, No. 4, 2001, pp. 1937-1955. [doi:10.1063/1.1353198](https://doi.org/10.1063/1.1353198)
- [13] A. Rosenzwaig, "Photo Acoustic and Photo Acoustic Spectroscopy," John Wiley and Sons, New York, 1980.
- [14] C. Brand, A. Winkler, P. Hess, A. Miklos, Z. Bozoki and J. Sneider, "Pulsed-laser Excitation of Acoustic Modes in Open High-Q Photo Acoustic Resonators for Trace Gas Monitoring: Results for C₂H₄," *Applied Optics*, Vol. 34, No. 18, 1995, pp. 3257-3266. [doi:10.1364/AO.34.003257](https://doi.org/10.1364/AO.34.003257)
- [15] P. M. Morse and K. U. Ingard, "Theoretical Acoustics," Princeton University Press, Princeton, New Jersey, 1986.
- [16] A. Karbach and P. Hess, "Photo Acoustic Signal in a Cylindrical Resonator: Theory and Laser Experiments for CH₄ and C₂H₄," *Journal of chemistry Physics*, Vol. 84, 1986, p. 2945. [doi:10.1063/1.450809](https://doi.org/10.1063/1.450809)
- [17] A. Miklos, P. Hess, A. Mohacsi, J. Sneider, S. Kamm and S. Schafer, "Photo Acoustic and Photo Theraml Phenomena," 10th *International Conference*, edited by I. F. Scudier and M. Bertolotti, AIP, Woodbury, New Jersey, 1999.